Electronic Supplementary Material (ESI) for Physical Chemistry Chemical Physics.

Organic acid formation in the gas-phase ozonolysis of α,β-unsaturated ketones

- Supporting Information -

N. Illmann, I. Patroescu-Klotz, and P. Wiesen

Table of Contents

A. Quantification and supplementary yield plots 2
B. PTR-ToF-MS data analysis 4
C. In situ generation and identification of peracids 6
1. Experimental 6
2. Results and discussion 7
D. Analysis of the RO_2 reactions 11
E. Overall error analysis 14
References 17

A. Quantification and supplementary yield plots

Table S1 Absolute and integrated absorption cross sections (base 10) used for the quantification via FTIR spectroscopy.

Species	Range / cm^{-1}	Integrated cross section / cm $molecule^{-1}$	Absolute cross section / cm^2 $molecule^{-1}$	Reference
Acetaldehyde	1761		$(1.7 \pm 0.1) \times 10^{-19}$	b
Ethyl hydroperoxide	2992		$(8.1 \pm 0.4) \times 10^{-20}$	b
Ethyl vinyl ketone	1768–1660	$(8.2 \pm 0.6) \times 10^{-18}$		a
Formaldehyde	1820–1660	$(5.5 \pm 0.3) \times 10^{-18}$		b
Formic acid	1840–1704	$(2.6 \pm 0.5) \times 10^{-17}$		b
Formic anhydride	1822		$(2.6 \pm 0.4) \times 10^{-19}$	b
Formic propionic anhydride	1824–1762	$(2.6 \pm 0.3) \times 10^{-17}$		b
Propionic acid	1880–1710	$(1.6 \pm 0.1) \times 10^{-17}$		a

[a] Determined within this work, [b] Wuppertal laboratory database.

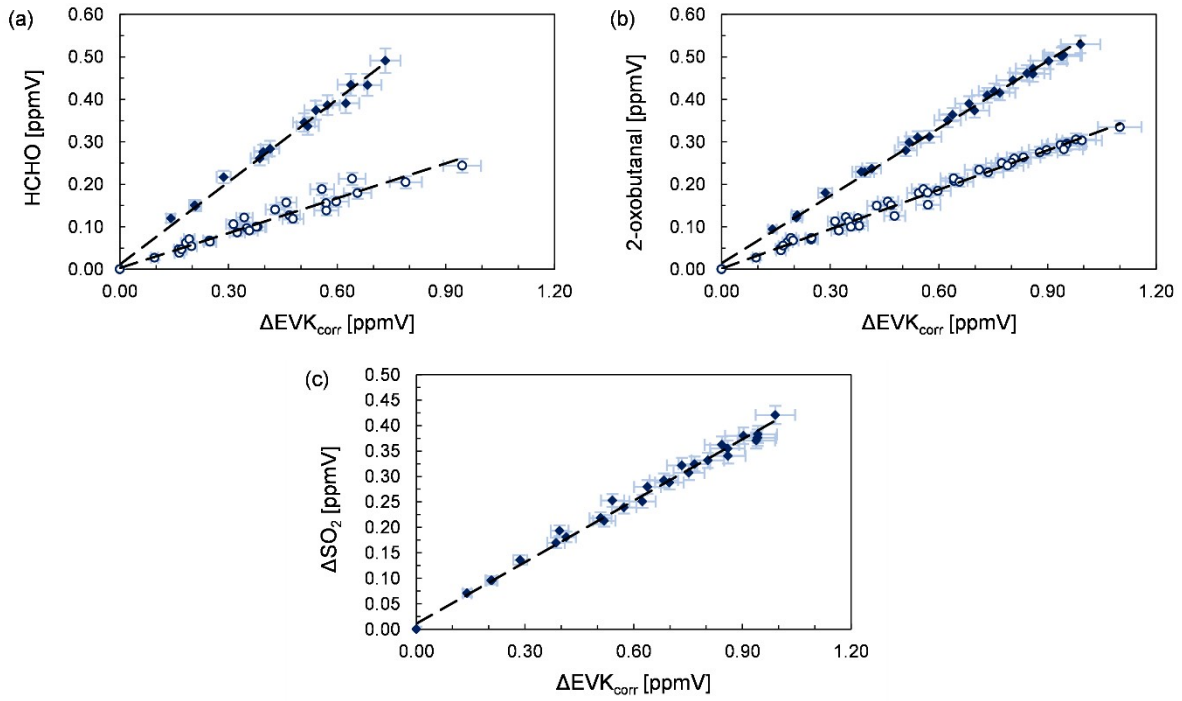

Fig. S1 Yield plots for (a) HCHO, and (b) 2-oxobutanal in the absence (open circles) and presence (filled diamonds) of SO_2, and (c) the consumption of SO_2 *vs.* the consumption of EVK. The error bars represent the respective precision errors.

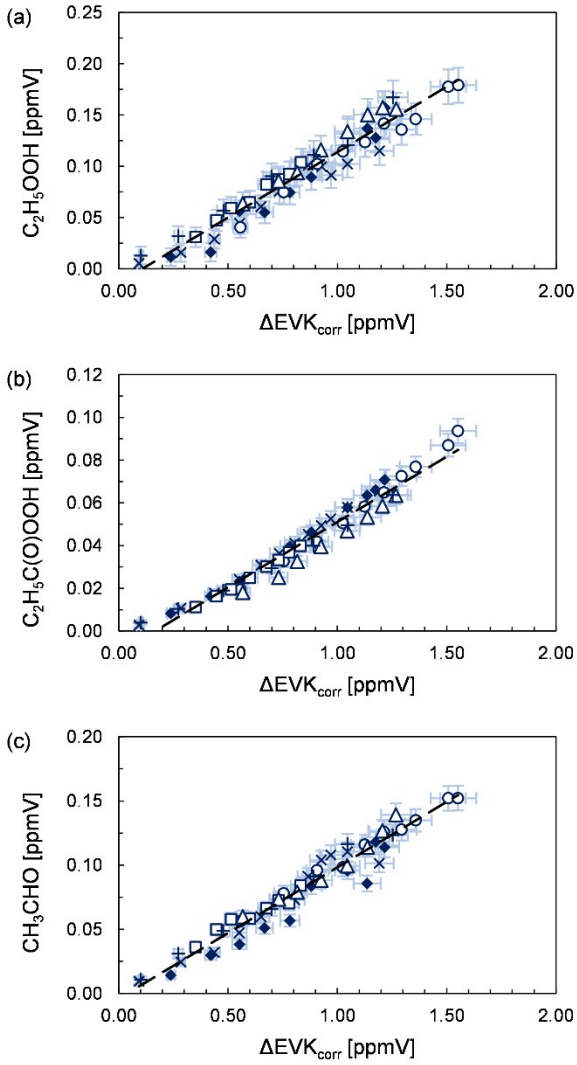

Fig. S2 Yield plots obtained for (a) ethyl hydroperoxide, (b) perpropionic acid, and (c) acetaldehyde, respectively, in the absence of SO_2. Different experimental runs are denoted by different symbols. The error bars represent a precision error as a combination of a relative error plus the corresponding detection limit under the experimental conditions.

B. PTR-ToF-MS data analysis

In each experiment (in the absence of SO_2), the PTR-ToF-MS data show the formation of species resulting in signals at *m/z* 31, 45, 47, 57, 59, 75, 87 and 91. Representative time profiles for all signals are shown in Fig. S4. The assignment to species is summarized in Tab. S2.

The formation of HCHO is confirmed by the increase of the *m/z* 31 signal (Fig S3). 2-Oxobutanal formation is strongly indicated by the evolution of the *m/z* 87 signal (Fig. S3) corresponding to protonated 2-oxobutanal ($C_4H_7O_2^+$, $[M–H]^+$). A *m/z* 59 signal, following a similar evolution (Fig. S4), is observed. For the structural analogue oxoaldehyde methyl glyoxal, beside the $[M–H]^+$ signal at *m/z* 73, fragment ions were reported at *m/z* 45 ($C_2H_5O^+$), which corresponds to a loss of CO.[1] Accordingly, the *m/z* 59 signal is likely a fragment ion of 2-oxobutanal ($C_3H_7O^+$). At the same time, methyl ketene, as suggested in the ozonolysis mechanism, might contribute to *m/z* 59.

The formation of formic acid is possibly supported by the evolution of the *m/z* 47 signal ($CH_3O_2^+$). In separate control experiments we observed that acetic anhydride is found solely as *m/z* 61 signal ($C_2H_5O_3^+$) suggesting anhydrides to appear exclusively as $[M–H]^+$ of their corresponding acid. Given that both formic anhydride (FA) and formic propionic anhydride (FPA) are observed in the FTIR spectra, the presence of the *m/z* 47 signal is probably mainly a consequence of the anhydride formation.

The proton-transfer reaction of peracetic acid was shown to produce mainly (≈ 90 %) protonated acetic acid,[2] which hence interferes with acetic acid at *m/z* 61 ($C_2H_5O_2^+$). A similar behaviour is likely for perpropionic acid, the expected dominant mass signal being *m/z* 75 ($C_3H_7O_2^+$). Due to the formation of formic propionic acid in the reaction system, the increase of the *m/z* 75 signal is not an unequivocal proof for the peracid. However, although much less intense (by a factor of ≈ 10^2), an increase is observed also for the *m/z* 91 ion, which could result from the protonated perpropionic acid.

The formation of ethyl hydroperoxide was clearly observed in the FTIR spectra. However, no signal was detected at *m/z* 63, corresponding to the protonated hydroperoxide ($C_2H_7O_2^+$). The fragment ion ($C_2H_5O^+$), built upon elimination of H_2O, interferes with acetaldehyde at *m/z* 45. Hence, although the evolution of the *m/z* 45 ion supports the FTIR data, a differentiation between the contribution of acetaldehyde and an ethyl hydroperoxide fragment is not possible.

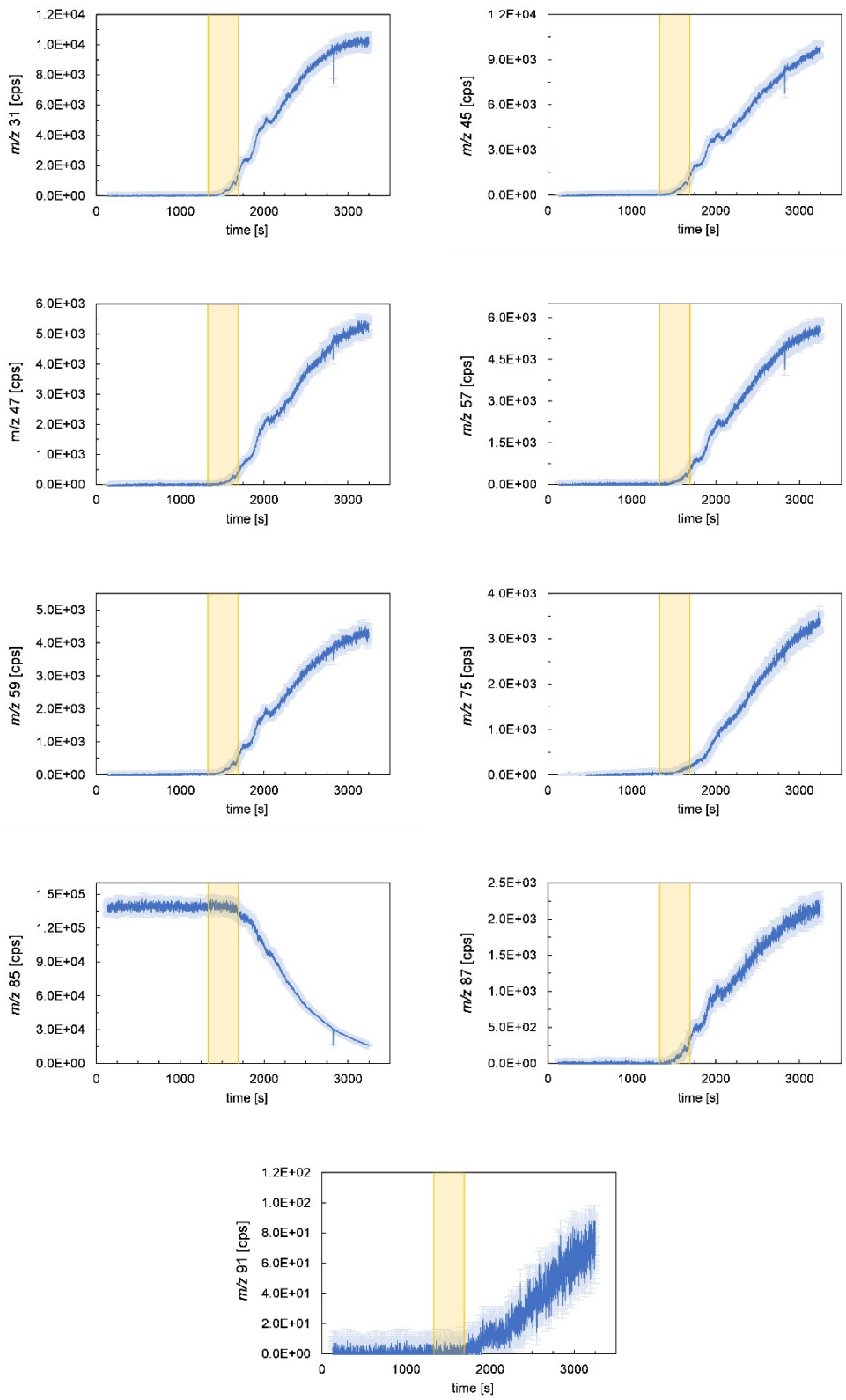

Fig. S3 Time profiles for *m/z* 31, 45, 47, 57, 59, 75, 85, 87, and 91 (dark blue) from a single EVK + O_3 experiment without sCI scavenger. The error bars (pale blue) represent the precision error. The pale yellow range marks the time of the ozone addition.

Table S2 Mass signals observed in the EVK + O_3 experiments, elemental composition and assigned species.

m/z	composition	Assigned species
31.018	CH_3O^+	HCHO
45.034	$C_2H_5O^+$	Acetaldehyde, Ethyl hydroperoxide (fragment)
47.013	$CH_3O_2^+$	Formic acid, Formic anhydride, Formic propionic anhydride
57.034	$C_3H_5O^+$	Methyl ketene or Propionyl
59.050	$C_3H_7O^+$	Propionaldehyde, 2-Oxobutanal (fragment)
75.045	$C_3H_7O_2^+$	Perpropionic acid, Formic propionic anhydride
87.045	$C_4H_7O_2^+$	2-Oxobutanal
91.040	$C_3H_7O_3^+$	Perpropionic acid

C. In situ generation and identification of peracids

1. Experimental

Infrared spectral features of peracetic acid (= peroxyacetic acid) and perpropionic acid (= peroxypropionic acid) were generated by the irradiation ($I_{max.}$ at 360 nm) of acetaldehyde/methanol/Cl_2 and propionaldehyde/methanol/Cl_2 mixtures in synthetic air, respectively, in both the 480 L and 1080 L chamber. The current set-up of the 480 L chamber is described in detail elsewhere.[3] Given that both the acetaldehyde + Cl and the propionaldehyde + Cl reaction proceed nearly exclusively via the abstraction of the aldehydic H atom, the respective RO_2 radicals are generated as follows:

$$Cl_2 + h\nu \rightarrow 2\ Cl \quad \text{(R1)}$$

$$RC(O)H + Cl + O_2 + M \rightarrow RC(O)O_2 + HCl + M^* \quad \text{(R2)}$$

In order to favour $RO_2 + HO_2$ reactions, the level of HO_2 is increased due to CH_3OH + Cl and the subsequent reaction sequence:

$$CH_3OH + Cl \rightarrow CH_2OH + HCl \quad \text{(R3)}$$

$$CH_2OH + O_2 \rightarrow HCHO + HO_2 \quad \text{(R4)}$$

$$HCHO + Cl \rightarrow HCO + HCl \quad \text{(R5)}$$

$$HCO + O_2 \rightarrow CO + HO_2 \quad \text{(R6)}$$

The $[HO_2]/[RO_2]$ ratio can be adjusted by the initial [aldehyde]/$[CH_3OH]$ ratio. Accordingly, the initial mixing ratios were set at 1.6–4.4 ppmV for acetaldehyde (Sigma Aldrich, > 99.5 %),

1.1–7.3 ppmV for propionaldehyde (Sigma Aldrich, 97 %), 1.9–16 ppmV for methanol (Sigma Aldrich, 99.9 %) and 1.9–21 ppmV for Cl_2 (Air Liquide, 99.8 %).

2. Results and discussion

Among RO_2 + HO_2 reactions the acetyl peroxy radical + HO_2 system is one of the most investigated reactions and reasonably well characterized.[4-11] The reported studies performed in simulation chambers were conducted mainly by irradiating acetaldehyde/methanol/Cl_2 mixtures.[6,7,10] Therefore, the in situ generation of peracetic acid was chosen to test the experimental set-up. All experiments were observed up to a maximum consumption of 60 – 70 % of the initial acetaldehyde. In order to promote RO_2 + HO_2 rather than RO_2 + RO_2 reactions, the initial aldehyde concentration was kept always lower than $[CH_3OH]_0$. In all experiments, significant amounts of hydrogen peroxide (H_2O_2) are formed. Since this can be rationalized through the HO_2 self-reaction, it indicates the HO_2 level to be near the upper experimental limit. In the case of acyl peroxy radicals, the RO_2 + HO_2 reaction was reported[6] to proceed through 3 different channels:

$$RC(O)O_2 + HO_2 \rightarrow RC(O)OOH + O_2 \quad \text{(R7a)}$$

$$RC(O)O_2 + HO_2 \rightarrow RC(O)OH + O_3 \quad \text{(R7b)}$$

$$RC(O)O_2 + HO_2 \rightarrow RC(O)O + OH + O_2 \quad \text{(R7c)}$$

Accordingly, both peracetic acid and acetic acid are formed in the $CH_3C(O)H/CH_3OH/Cl_2$ system. The alkoxy radical (R7c) eliminates CO_2 to yield a methyl radical, that is immediately converted into a methyl peroxy radical (CH_3O_2). The CH_3O_2 further chemistry evolves into methyl hydroperoxide and HCHO through the reaction with HO_2 and, possibly, into HCHO and CH_3OH through the CH_3O_2 self-reaction. However, if RO_2 + RO_2 plays a role, the cross reaction of the alkyl peroxy and acyl peroxy radical is about a factor of 10^2 faster and proceeds as follows[12]

$$RC(O)O_2 + R'O_2 \rightarrow RC(O)O + R'O + O_2 \quad \text{(R8a)}$$

$$RC(O)O_2 + R'O_2 \rightarrow RC(O)OH + R_{-H}'(O)H + O_2 \quad \text{(R8b)}$$

In consequence, after the subtraction of the reaction sequence's products (acetic acid, O_3, CO_2, CH_3OOH, HCHO) as well as CH_3OH, HCHO, HC(O)OH, H_2O_2 and HCl, the residual

spectrum of such a reaction mixture should correspond to peracetic acid. Trace (b) of Fig. S4 shows a residual spectrum obtained from an irradiated $CH_3C(O)H/CH_3OH/Cl_2$ mixture, which is in excellent agreement with a reference spectrum of peracetic acid from the Wuppertal laboratory database, presented in trace (a). The residual spectrum shows additional small curvatures centred at 1150 cm^{-1} and 1050 cm^{-1}. However, this can be partly explained by artefacts due to the subtraction of high amounts of methanol, those absorption dominates at 1050 cm^{-1}. Additionally, a curvature of the baseline was observed in this region in some experiments, which might also be built artificially due to the subtraction process. Despite this, the experimental set-up was proven successful in obtaining the spectral features of peracids, as shown in Fig. S4.

The experiments irradiating $C_2H_5C(O)H/CH_3OH/Cl_2$ mixtures were performed until a maximum consumption of 30–60 % of propionaldehyde. Similarly to the irradiation of mixtures containing acetaldehyde, H_2O_2 formation was also observed. This indicates a high HO_2 level in the experimental system, necessary to promote the RO_2 + HO_2 reactions. According to the reactions (R7a)–(R7c) perpropionic acid, propionic acid and $C_2H_5C(O)O$ radicals are formed from the $C_2H_5C(O)O_2$ + HO_2 reaction. The existence of all 3 reaction channels has been proven previously by Hasson et al.[13] However, although FTIR spectroscopy has also been used in the Hasson et al. study,[13] the peracid was quantified with HPLC and up to date no IR spectrum was reported for perpropionic acid.

As discussed above, in the presence of O_2, the $C_2H_5C(O)O$ radical eliminates CO_2 to form the ethyl peroxy radical. Similarly to methyl peroxy radical, the ethyl peroxy radical further chemistry yields ethyl hydroperoxide and possibly acetaldehyde. The residual spectrum assigned to perpropionic acid was obtained by subtraction of the spectral features of the following species: propionaldehyde, methanol, HCHO, formic acid, CO_2, propionic acid, ethyl hydroperoxide, O_3, acetaldehyde, peracetic acid, H_2O_2, and HCl. The perpropionic acid spectrum is presented in Fig. S4, trace (c).

The spectrum contains characteristic absorption bands centred at 3303, 1760, 1450, 1180 and 880 cm^{-1}, which are nearly identical to the absorption features of peracetic acid, and were assigned on the basis of well acknowledged rules. The position of the absorption centred at 3303 cm^{-1} is identical to the peracetic acid spectrum. This absorption band is assigned to the strong OH stretching vibration, which is significantly shifted towards lower wavenumbers compared to free OH stretching vibrations of alcohols and acids, for instance. This is attributed to intramolecular H-bonding, which lowers the bond strength and subsequently the wavenumber of the absorption band. In the case of peracids, this results in the formation of

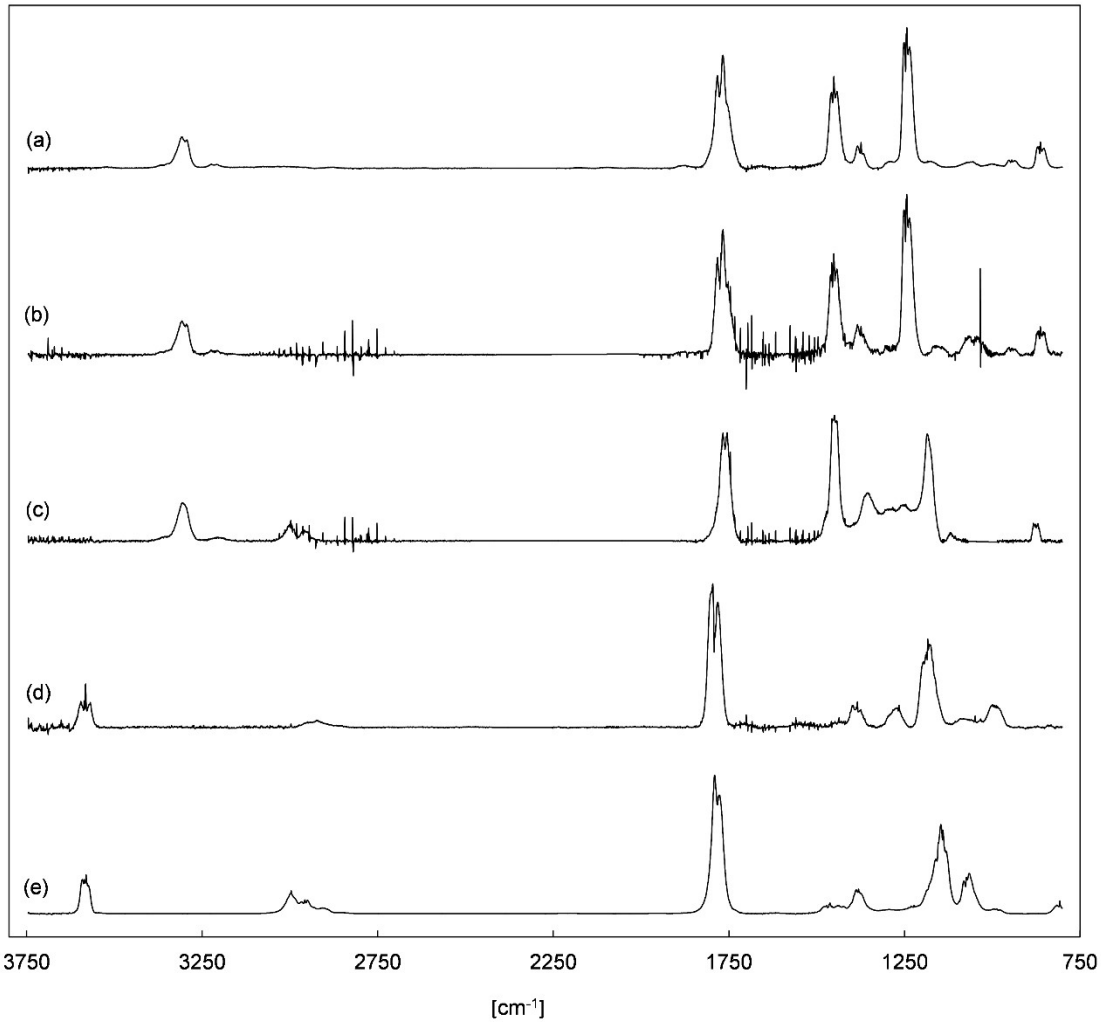

Fig. S4 (a) Reference spectrum of peracetic acid (peroxyacetic acid), (b) residual spectrum corresponding to peracetic acid generated in a $CH_3C(O)H/CH_3OH/Cl$ mixture, (c) residual spectrum assigned to perpropionic acid generated in a $C_2H_5C(O)H/CH_3OH/Cl$ mixture, (d) spectrum of acetic acid, and (e) spectrum of propionic acid. The spectra were straightened in the range 2400–1900 cm^{-1}.

stable five-membered rings.[14] This characteristic absorption is therefore an undoubted proof for the presence of a peracid. The residual spectrum contains an absorption band at 1450 cm^{-1}, again similar to the peracetic acid spectrum, which is assigned to the OH bending vibration. The absorption bands centred at 1760 cm^{-1} and 1180 cm^{-1} are attributed to the C=O and C-O stretching vibration. Both absorption features are shifted towards lower wavenumbers compared to the peracetic acid spectrum where a larger shift is observed for the C-O stretching vibration (from 1245 cm^{-1} to 1180 cm^{-1}). Trace (d) and trace (e) of Fig. S4 depict reference spectra of gas-phase acetic acid and propionic acid, those absorption bands show the same

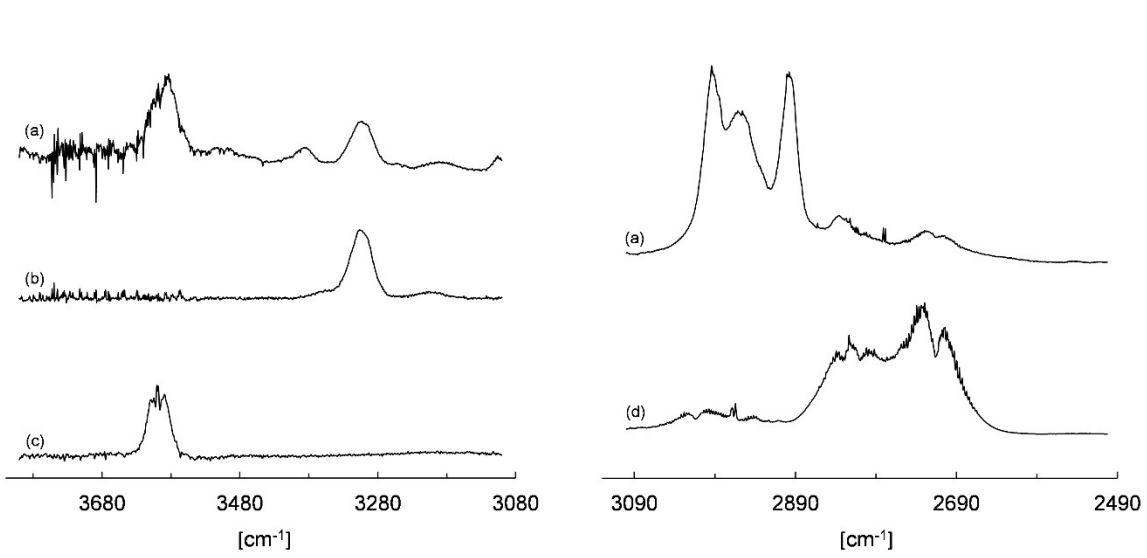

Fig. S5 (a) Spectrum of an EVK + O_3 experiment, collected after an EVK consumption of about 70 %, after subtraction of H_2O, EVK, HCHO, HC(O)OH, and 2-oxobutanal, and reference spectra of (b) perpropionic acid, (c) ethyl hydroperoxide, and (d) acetaldehyde, respectively.

behaviour for the C=O and C-O stretching vibration. Therefore, all these findings give confidence in attributing the absorption features of the residual spectrum to perpropionic acid.

Trace (a) of Fig. S5 shows residual absorption features from an evaluated ozonolysis experiment performed in the absence of SO_2. The spectrum was collected after an EVK consumption of about 70 %. H_2O, EVK, HCHO, HC(O)OH, and 2-oxobutanal were subtracted at this stage. Apparently, a product is formed with a clear absorption band centred on about 3303 cm^{-1}, which appears almost identical to the spectrum assigned to perpropionic acid (trace (b) of Fig. S5). In addition, the *m/z* 91 signal supports that perpropionic acid is formed, as discussed above. There is no obvious pathway forming acetyl peroxy radicals, which could finally result in the formation of peracetic acid. In addition, neither the PTR mass spectra nor other spectral ranges of the FTIR spectra support that peracetic acid is formed in the reaction system. All this are strong arguments that perpropionic acid is formed in the EVK + O_3 reaction.

D. Analysis of the RO_2 reactions

Perpropionic acid formation can solely be rationalized through the reaction of the propionyl peroxy radical ($C_2H_5C(O)O_2$) with HO_2. Up to now, this reaction has only been investigated by Hasson et al.[13] who reported branching ratios of 0.35 ± 0.1, 0.25 ± 0.1, and 0.4 ± 0.1 for the pathways yielding perpropionic acid, propionic acid and ethyl peroxy radicals ($C_2H_5O_2$), respectively. The latter radical itself reacts with HO_2 to form ethyl hydroperoxide. The acetaldehyde formation can only proceed via RO_2 + RO_2 reactions. Both, the $C_2H_5C(O)O_2$ + $C_2H_5O_2$ reaction and the $C_2H_5O_2$ self-reaction produce eventually acetaldehyde. Since the rate coefficient of the self-reaction is 10^2 times smaller than that for the $C_2H_5C(O)O_2$ + $C_2H_5O_2$ reaction,[15,16] the $C_2H_5O_2$ self-reaction is expectedly negligible in the present experiments (without SO_2). This is supported by the fact that neither FTIR spectra nor PTR mass spectra indicate the formation of ethanol, which is a specific product of the $C_2H_5O_2$ self-reaction.

The rate coefficient of the $C_2H_5C(O)O_2$ self-reaction is comparable to the RO_2 cross-reaction.[15] Hence, the self-reaction increases the level of ethyl peroxy radicals in the experiments due to the conversion from $C_2H_5C(O)O_2$ into $C_2H_5O_2$ radicals. In the absence of SO_2, the acetaldehyde yield was found to be the same as the ethyl hydroperoxide yield within the assigned uncertainties. Therefore, about 50 % of the ethyl peroxy radicals react with HO_2, whereas the rest reacts with propionyl peroxy radicals.

About 20 % of $C_2H_5C(O)O_2$ + $C_2H_5O_2$ reaction results also in propionic acid, those formation was not observed in the absence of SO_2 due to the fast reaction of organic acids with sCI.

In order to prove if the temporal behaviour of acetaldehyde, ethyl hydroperoxide, propionic acid and perpropionic acid can be described solely through the known RO_2 reactions, the temporal evolution of the reaction products was simulated following the approach described recently in the literature.[3,17] Table S3 summarizes the reaction sequences employed to describe the system. Model runs were performed assuming the EVK + O_3 reaction to form initially either $C_2H_5C(O)O_2$ or $C_2H_5C(O)O_2$ and $C_2H_5O_2$ radicals. Experimental and simulated time profiles for a representative experiment are shown in Fig. S6.

A major uncertainty of the simulations is [HO_2], given that the HO_2 concentration could not be determined experimentally. The value is adjusted mainly by reproducing concurrently the experimental time profiles of the peroxides. However, when only $C_2H_5C(O)O_2$ radicals are formed promptly from EVK + O_3, an estimation of the overall $C_2H_5C(O)O_2$ radical yield is given by the sum of the acetaldehyde, ethyl hydroperoxide and perpropionic acid yield. The

Table S3 Reaction sequence used for modelling the temporal behaviour of acetaldehyde, ethyl hydroperoxide, and perpropionic acid.

Reaction		Branching ratio	Rate coefficient [a]
(R9a) [b]	CH_2=CHC(O)C_2H_5 + O_3 → $C_2H_5C(O)O_2$		[c]
(R9b) [b]	CH_2=CHC(O)C_2H_5 + O_3 → $C_2H_5O_2$		[c]
(R10)	$C_2H_5C(O)O_2$ + HO_2 → products		2.0×10^{-11} [d]
(R10a)	$C_2H_5C(O)O_2$ + HO_2 → $C_2H_5C(O)OOH$ + O_2	0.35 [e]	
(R10b)	$C_2H_5C(O)O_2$ + HO_2 → $C_2H_5C(O)OH$ + O_3	0.25 [e]	
(R10c)	$C_2H_5C(O)O_2$ + HO_2 (+ O_2) → $C_2H_5O_2$ + OH + O_2 + CO_2	0.40 [e]	
(R11)	2 $C_2H_5C(O)O_2$ (+ O_2) → 2 $C_2H_5O_2$ + O_2 + 2 CO_2		1.7×10^{-11} [f]
(R12)	$C_2H_5C(O)O_2$ + $C_2H_5O_2$ → products		1.2×10^{-11} [f]
(R12a)	$C_2H_5C(O)O_2$ + $C_2H_5O_2$ (+ O_2) → $C_2H_5O_2$ + CO_2 + $CH_3C(O)H$ + HO_2 + O_2	0.8 [f]	
(R12b)	$C_2H_5C(O)O_2$ + $C_2H_5O_2$ → $C_2H_5C(O)OH$ + $CH_3C(O)H$ + O_2	0.2 [f]	
(R13)	$C_2H_5O_2$ + HO_2 → C_2H_5OOH + O_2		6.9×10^{-12} [f]
(R14)	2 $C_2H_5O_2$ → products		7.6×10^{-14} [f]
(R14a)	2 $C_2H_5O_2$ (+ O_2) → 2 $CH_3C(O)H$ + 2 HO_2 + O_2	0.37 [f]	
(R14b)	2 $C_2H_5O_2$ → $CH_3C(O)H$ + C_2H_5OH + O_2	0.63 [f]	

[a] In [cm^3 $molecule^{-1}$ s^{-1}], [b] either a prompt source of $C_2H_5C(O)O_2$ (R9a) or $C_2H_5C(O)O_2$ and $C_2H_5O_2$ radicals (R9a + R9b) was considered, [c] the radical source was included according to the experimental first-order loss of EVK, [d] the rate coefficient was assumed to be the same as the IUPAC recommended value for the $CH_3C(O)O_2$ + HO_2 reaction, [e] Hasson et al.[27], [f] IUPAC recommended values (2021).

temporal profiles of both acetaldehyde and ethyl hydroperoxide, whose quantification errors are much smaller than for perpropionic acid, were found to be very sensitive to the overall $C_2H_5C(O)O_2$ radical yield and [HO_2]. Though, adjusting both [HO_2] and the overall $C_2H_5C(O)O_2$ radical yield allows a simultaneous fit for all temporal profiles within the uncertainties of the experimentally determined product yields. On average, the experimental time profiles are reproduced using a $C_2H_5C(O)O_2$ radical yield of 0.39 and [HO_2] ≈ 2.3×10^{10} cm^{-3}. Under these conditions propionic acid were formed with a yield of about 0.07, originating from $C_2H_5C(O)O_2$ + $C_2H_5O_2$ and $C_2H_5C(O)O_2$ + HO_2.

When a prompt source of $C_2H_5O_2$ radicals from the EVK + O_3 reaction is included, a match of all time profiles is achieved only for the lower accuracy range of the perpropionic acid data (Fig. S6). Accordingly, the overall $C_2H_5C(O)O_2$ radical yield is lower (about 0.30) than without considering a potentially prompt source of $C_2H_5O_2$ radicals, although in all model runs the $C_2H_5O_2$ source was found to be a factor of ≈ 5 smaller than the $C_2H_5C(O)O_2$ source. Under these conditions, the simulation generates a slightly lower propionic acid yield (0.05). For both scenarios, the simulations predict an ethanol level well below 1 ppbV at the end of each experiment. This, in turn, is below the detection limit of the instrument under the conditions used for the experiments.

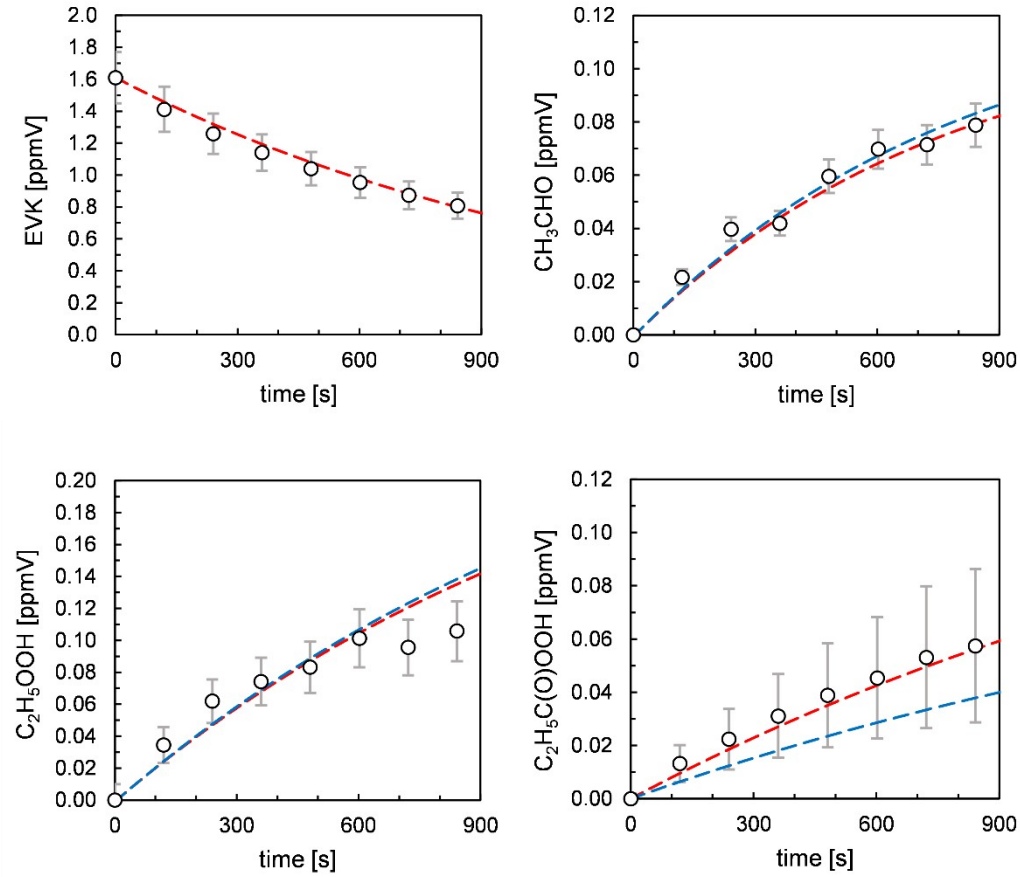

Fig. S6 Experimental (open circles) and simulated time profiles (dashed lines) of ethyl vinyl ketone (EVK), acetaldehyde (CH_3CHO), ethyl hydroperoxide (C_2H_5OOH), and perpropionic acid ($C_2H_5C(O)OOH$) obtained from an experiment performed in the absence of SO_2. The error bars represent the respective accuracy error. Since the addition of ozone cannot be simulated, t = 0 was set to the time, when the first FTIR spectrum was recorded after the ozone addition. Accordingly, the amount of products present in the first spectrum was subtracted from all data points. The simulations were performed assuming $[HO_2] = 2.7 \times 10^{10}$ cm^{-3} and a $C_2H_5C(O)O_2$ yield of 0.42 (scenario 1, red) or $[HO_2] = 2.2 \times 10^{10}$ cm^{-3}, a $C_2H_5C(O)O_2$ yield of 0.32 and a $C_2H_5O_2$ yield of 0.07 (scenario 2, blue).

Although this modelling approach is rather uncertain, since the major criticism - that $[HO_2]$ is actually not known - remains, there is one important observation to be made. The fact that for this type of experiments the temporal evolution of acetaldehyde, ethyl hydroperoxide and perpropionic acid is reproduced with the same set of parameters, which are experimentally plausible, suggests that there is no reason to argue against their time profiles being properly described by the peroxy radical reaction sequence as listed in Table S3. At the same time it is not possible to conclude whether the ethyl peroxy radical evolves solely from the propionyl peroxy radical further chemistry or also promptly from the CI chemistry. Nevertheless, the present results hint at the propionyl peroxy radical being the dominant RO_2.

Since in the presence of SO_2 no hydroperoxides could be quantified, this is an indication that the RO_2 further chemistry is dominated by RO_2 + RO_2 reactions in this type of experiment. Although all possible RO_2 + RO_2 reactions shift the reaction system towards acetaldehyde formation, the acetaldehyde yield is about a factor of 2 smaller in the presence of SO_2 than the sum of the acetaldehyde, ethyl hydroperoxide and perpropionic acid yield in the absence of SO_2. This indicates a much lower RO_2 level when the sCIs are scavenged with SO_2 and hence their origin from both chemically activated and stabilized CIs. However, in this set-up it is not possible to decipher precisely between the contribution of the $C_2H_5O_2$ self-reaction and the $C_2H_5C(O)O_2$ + $C_2H_5O_2$ reaction towards acetaldehyde formation. Since, contrary to ethyl hydroperoxide, the formation of perpropionic acid in the presence of SO_2 is at least suggested by the FTIR data, this might argue that the propionyl peroxy radical remains the dominant RO_2 radical. Further, the formation of ethanol, following the $C_2H_5O_2$ self-reaction, was not supported by the FTIR spectra in any of the experiments.

Due to the absence of quantifiable amounts of hydroperoxides, we were not able to adjust [HO_2] in the model as we did for the experiments without SO_2 added. However, we used the model to figure out the propionic acid/acetaldehyde ratio by variation of the RO_2 yield and [HO_2] considering the fact that an acetaldehyde yield of about 15 % was observed experimentally. Using the average RO_2 yields found for the experiments in the absence of SO_2, we obtained an upper limit of 0.5 for the propionic acid/acetaldehyde ratio considering the uncertainties on the acetaldehyde yield. Lowering the RO_2 yield in the simulation requires a lower HO_2 concentration in order to match the acetaldehyde yield. This, in turn, decreases the propionic acid/acetaldehyde ratio. At the same time, an increase in the $C_2H_5O_2/C_2H_5C(O)O_2$ ratio (scenario 2) lowers also the propionic acid/acetaldehyde ratio. Apparently, the simulations suggest the propionic acid/acetaldehyde ratio to be well below the experimentally observed ratio (1.1 ± 0.2) evidencing an additional source of propionic acid in the reaction system.

E. Error analysis

The experimental results suggest a 1:1 ratio for the decomposition of the primary ozonide. However, the sum of the primary carbonyls is well below 100 %. It appears that in the present investigation the POZ decomposition accounts solely for about 57 ± 14 % of the EVK + O_3 reaction. We did not find any hint for products suggesting pathways competitive to the POZ formation, e. g. the formation of an epoxide. At the same time, the increase of the HCHO + 2-oxobutanal yield when SO_2 is added to the system is larger than suggested from the SO_2

consumption. While a smaller increase appears plausible once the sCI + SO_2 reaction exhibits additional pathways (e. g. the formation of stable sCI-SO_2 adducts partitioning into the aerosol phase), the inverse case suggests rather quantification errors or secondary processes not considered in the analysis.

One might intuitively think that this indicates an overestimation of the EVK consumption. Though, even after re-analysis of the calibration data and additional control experiments there is no indication for an erroneous infrared cross section. A hypothetically secondary loss process might be the reaction of EVK with sCIs, lowering the product yields in the absence of SO_2. At least for the structural analogue methyl vinyl ketone (MVK) it was shown that, under experimental conditions similar to the present study, the observed kinetics of MVK + O_3 was not affected by the reaction of the unsaturated ketone with CIs.[18] It is therefore reasonable to assume that EVK + O_3 exhibits the same behaviour.

Our HCHO absorption cross section is in excellent agreement with literature data. The high linearity of the yield plots (Fig. S1) rules out an underestimation of the HCHO yield due to a potential wall loss. Alternatively, a conceivable loss process of HCHO might be its reaction with HO_2 (R15),[19,20] which is known to become likely relevant under higher radical concentrations present in chamber experiments.

$$HCHO + HO_2 \rightarrow HOCH_2O_2 \quad \text{(R15)}$$

$$HOCH_2O_2 \rightarrow HCHO + HO_2 \quad \text{(R16)}$$

The $HOCH_2O_2$ further chemistry might evolve, for instance, into formic acid (HC(O)OH) formation via the RO_2 self-reaction or the reaction with HO_2. In principle, the level of HO_2 is reasonably high mainly due to the conversion of OH into HO_2 by carbon monoxide.

When we simulate the temporal evolution of HCHO for a simplified reaction system observing the reactions (R15), (R16), $HOCH_2O_2$ + $HOCH_2O_2$ and $HOCH_2O_2$ + HO_2, it is found that HO_2 levels about a factor of 40–50 larger than concluded in Sect. D are necessary in order to observe a measurable influence on HCHO. Although the value obtained for [HO_2] provides just a rough estimate, a factor of 40–50 is far beyond the uncertainties and experimentally implausible. The observed HCHO yield is therefore not expectedly affected by a secondary consumption of HCHO by HO_2.

Assuming HCHO to be correct, the 2-oxobutanal yield would be underestimated by a factor of about 2.5 in order to match the 100 % primary carbonyl yield in the absence of SO_2. A 20 % error, which we considered in our error calculation, appears reasonable due to the semi-

quantitative approach we used to quantify 2-oxobutanal. However, it is physically not plausible that the cross sections of the carbonyl absorptions of 2-oxobutanal and methyl glyoxal diverge by a factor of 2.5. At the same time, the linearity of the yield plots (Fig. S1) rules out a large influence of wall losses on the 2-oxobutanal yield.

Overall, we do not find a conclusive explanation for the lower than expected primary carbonyl yields in the absence of SO_2. Since quantification errors were ruled out, we can only imagine a secondary process consuming the primary carbonyls in the absence of SO_2. Further investigations are required to identify this process.

References

1 M. Müller, M. Graus, A. Wisthaler, A. Hansel, A. Metzger, J. Dommen, and U. Baltensperger, Analysis of high mass resolution PTR-TOF mass spectra from 1,3,5-trimethylbenzene (TMB) environmental chamber experiments, *Atmos. Chem. Phys*., 2012, **12**, 829–843.

2 P. Španěl, A. M. Diskin, T. Wang, and D. Smith, A SIFT study of reactions of H_3O^+, NO^+, and O_2^+ with hydrogen peroxide and peroxyacetic acid, *Int. J. Mass Spectrom*., 2003, **228**, 269–283.

3 N. Illmann, R. G. Gibilisco, I. G. Bejan, I. Patroescu-Klotz and P. Wiesen, Atmospheric oxidation of α,β-unsaturated ketones: kinetics and mechanism of the OH radical reaction, *Atmos. Chem. Phys*., 2021, **21**, 13667–13686.

4 H. Niki, P. D. Maker, C. M. Savage, and L. P. Breitenbach, FTIR Study of the Kinetics and Mechanism for Cl-Atom-Initiated Reactions of Acetaldehyde, *J. Phys. Chem*., 1985, **89**, 588–591.

5 O. Horie, and G. K. Moortgat, Reactions of $CH_3C(O)O_2$ radicals with CH_3O_2 and HO2 between 263 and 333 K. A product study, *J. Chem. Soc., Faraday Trans*., 1992, **88**, 3305–3312.

6 A. S. Hasson, G. S. Tyndall, and J. J. Orlando, A Product Yield Study of the Reaction of HO_2 Radicals with Ethyl Peroxy ($C_2H_5O_2$), Acetyl Peroxy ($CH_3C(O)O_2$), and Acetonyl Peroxy ($CH_3C(O)CH_2O_2$) Radicals, *J. Phys. Chem. A*, 2004, **108**, 5979–5989.

7 M. E. Jenkin, M. D. Hurley, and T. J. Wallington, Investigation of the radical product channel of the $CH_3C(O)O_2 + HO_2$ reaction in the gas phase, *Phys. Chem. Chem. Phys*., 2007, **9**, 3149–3162.

8 T. J. Dillon, and J. N. Crowley, Direct detection of OH formation in the reactions of HO_2 with $CH_3C(O)O_2$ and other substituted peroxy radicals, *Atmos. Chem. Phys*., 2008, **8**, 4877–4889.

9 C. B. M. Groß, T. J. Dillon, G. Schuster, J. Lelieveld, and J. N. Crowley, Direct Kinetic Study of OH and O_3 Formation in the Reaction of $CH_3C(O)O_2$ with HO_2, *J. Phys. Chem. A*, 2014, **118**, 974–985.

10 F. A. F. Winiberg, T. J. Dillon, S. C. Orr, C. B. M. Groß, I. Bejan, C. A. Brumby, M. J. Evans, S. C. Smith, D. E. Heard, and P. W. Seakins, Direct measurements of OH and other product yields from the $HO_2 + CH_3C(O)O_2$ reaction, *Atmos. Chem. Phys*., 2016, **16**, 4023–4042.

11 A. O. Hui, M. Fradet, M. Okumura, and S. P. Sander, Temperature Dependence Study of the Kinetics and Product Yields of the $HO_2 + CH_3C(O)O_2$ Reaction by Direct Detection of OH and HO_2 Radicals Using 2f-IR Wavelength Modulation Spectroscopy, *J. Phys. Chem. A*, 2019, **123**, 3655–3671.

12 G. S. Tyndall, R. A. Cox, C. Granier, R. Lesclaux, G. K. Moortgat, M. J. Pilling, A. R. Ravishankara, and T. J. Wallington, Atmospheric chemistry of small organic peroxy radicals, *J. Geophys. Res*., 2001, **106**, 12157.

13 A. S. Hasson, G. S. Tyndall, J. J. Orlando, S. Singh, S. Q. Hernandez, S. Campbell, and Y. Ibarra, Branching Ratios for the Reaction of Selected Carbonyl-Containing Peroxy Radicals with Hydroperoxy Radicals, *J. Phys. Chem. A*, 2012, **116**, 6264–6281.

14 P. A. Giguère, and A. Weingartshofer Olmas, A spectroscopic study of hydrogen bonding in performic and peracetic acids, *Can. J. Chem*., 1952, **30**, 821–830.

15 J.-P. Le Crâne, E. Villenave, M. D. Hurley, T. J. Wallington and J. C. Ball, Atmospheric Chemistry of Propionaldehyde: Kinetics and Mechanisms of Reactions with OH Radicals and Cl Atoms, UV Spectrum, and Self-Reaction Kinetics of $CH_3CH_2C(O)O_2$ Radicals at 298 K, *J. Phys. Chem. A*, 2005, **109**, 11837–11850.

16 A. C. Noell, L. S. Alconcel, D. J. Robichaud, M. Okumura and S. P. Sander, Near-Infrared Kinetic Spectroscopy of the HO_2 and $C_2H_5O_2$ Self-reactions and Cross-Reactions, *J. Phys. Chem. A*, 2010, **114**, 6983–6995.

17 N. Illmann, I. Patroescu-Klotz, and P. Wiesen, Biomass burning plume chemistry: OH-radical-initiated oxidation of 3-penten-2-one and its main oxidation product 2-hydroxypropanal, *Atmos. Chem. Phys*., 2021, **21**, 18557–18572.

18 P. Neeb, A. Kolloff, S. Koch, and G. K. Moortgat, Rate constants for the reactions of methylvinyl ketone, methacrolein, methacrylic acid, and acrylic acid with ozone, *Int. J. Chem Kinet*., 1999, **30**, 769–776.

19 I. Barnes, K. H. Becker, E. H. Fink, A. Reimer, F. Zabel, and H. Niki, FTIR spectroscopic study of the gas-phase reaction of HO_2 with H_2CO, *Chem. Phys. Lett*., 1985, **115**, 1–8.

20 B. Veyret, R. Lesclaux, M.-T. Rayez, J.-C. Rayez, R. A. Cox, and G. K. Moortgat, Kinetic and Mechanism of the Photooxidation of Formaldehyde. 1. Flash Photolysis Study, *J. Phys. Chem*., 1989, **93**, 2368–2374.